



Emergence of body waves from cross-correlation of short period seismic noise.

Piero Poli, Helle Pedersen, Michel Campillo

► To cite this version:

Piero Poli, Helle Pedersen, Michel Campillo. Emergence of body waves from cross-correlation of short period seismic noise.. *Geophysical Journal International*, 2012, Volume 188 (Issue 2), p. 549-558. 10.1111/j.1365-246X.2011.05271.x . hal-00706814

HAL Id: hal-00706814

<https://hal.science/hal-00706814>

Submitted on 11 Jun 2012

HAL is a multi-disciplinary open access archive for the deposit and dissemination of scientific research documents, whether they are published or not. The documents may come from teaching and research institutions in France or abroad, or from public or private research centers.

L'archive ouverte pluridisciplinaire **HAL**, est destinée au dépôt et à la diffusion de documents scientifiques de niveau recherche, publiés ou non, émanant des établissements d'enseignement et de recherche français ou étrangers, des laboratoires publics ou privés.

Emergence of body waves from cross-correlation of short period seismic noise

P. Poli¹, H. A. Pedersen¹, M. Campillo¹, and the POLENET/LAPNET Working Group

1-ISTerre, CNRS, universite' Joseph-Fourier, BP 53, 38041 Grenoble cedex 9, France

SUMMARY

Ambient noise correlation is now widely used in seismology to obtain the surface waves part of the Green's function. More difficult is the extraction of body waves from noise correlations. Using 42 temporary broad-band three components stations located on the northern part of fennoscandian region, we identify high frequency (0.5-2 Hz) body waves emerging from noise correlations for inter-station distances up to 550 km. The comparison of the noise correlations with earthquake data confirm that the observed waves can be interpreted as P and S waves reflected from the Moho. Because the crustal model of the area is well known, we also compared the noise correlations with synthetic seismograms, and found an excellent agreement between the travel times of all the observed phases. Polarization analysis provide a further arguments to confirm the observation of body waves.

Key words: Interferometry, Body waves, Wave propagation.

INTRODUCTION

The possible extraction of the Green's function through correlation of seismic noise has opened up for potentially new and exciting developments in seismic imaging and monitoring of the elastic properties in the Earth. The feasibility of the method is now understood through a series of theoretical developments (e.g. Weaver and Lobkis, 2001; Wapenaar, 2004; Roux et al. 2005b, Gouédard et al., 2008, De Verdière, 2011) and through

laboratory experiments (Weaver and Lobkis, 2001). Shapiro and Campillo demonstrated the feasibility of the method by extracting intermediate and long period surface waves on field data (Shapiro and Campillo, 2004), and numerous studies have now based imaging on the analysis of seismic surface waves extracted by noise correlations (e.g. Sabra et al., 2005b; Shapiro et al., 2005; Yang et al., 2007; Yao et al., 2008, Ritzwoller et al., 2011).

It is generally assumed that noise is related to surface activity, ranging from human activity at high frequency to the forcing of oceans and atmosphere at low frequency. In the absence of deep sources, and with uneven distribution of surface sources, the reconstruction of body waves relies on the energy that has been scattered at depth. Although with an energy smaller than the one of the surface waves locally radiated by the sources, the scattered body waves are present in actual seismograms acquired at the surface, as a part of the almost equipartitioned diffuse field observed for long lapse time (e.g Hennino et al., 2001, Campillo, 2006).

There should therefore be substantial hope of extracting the body wave part of the Green's function, albeit with a lower signal to noise ratio than the dominant surface waves. Body waves have indeed been reported from short distance range correlations. Roux (2005a) identified direct P waves from noise correlation, using data from a small array in California. Their noise derived P waves were linearly polarized, and with a velocity compatible with a known velocity model of the area. Draganov et al. (2009) used data from oil exploration to extract reflected P waves from shallow interfaces. Their observed body waves were in good agreement with the active source reflection response in the same area. Zhan et al. (2010) identified S reflected phases from the Moho interface at the critical distance in two shield areas. The S waves presented a striking agreement with earthquake data. On the contrary, the extraction of body waves over broader distance ranges has so far not been successful, even though such waves would be key for body wave tomography at crustal scale.

To study the possibility of recovering body waves over large distance ranges from seismic noise correlation, we processed one year of data acquired at POLENET/LAPNET seismological array (Kozlovskaya et al., 2006). This dataset is acquired by a seismic array including 42 broadband stations. The study area is part of the Precambrian northwestern segment of the East European Craton, and the crust is relatively well known from active seismic experiments (HUKKA, FIRE, FIRE4, POLAR), from which it is known that the velocity structure remains relatively simple and with limited lateral variations and a limited variation of Moho depth (Janik et al., 2007, and reference therein). The major seismic phases observed from active source experiments were PmP and SmS (Janik et al., 2007), while weak amplitudes were reported for mantle phases (Pn and Sn) and inter-crustal reflection (Pg and Sg). As body waves are expected to be strong and impulsive in a crust characterised by weak scattering and attenuation, the geological and such observations of strong PmP combined with weak crustal scattering and attenuation (Pedersen et al., 1991, Uski et al. 1996), are particularly promising elements for the extraction of body waves from noise correlations.

We firstly present the dataset and the data processing, after which we discuss the noise correlations and the fast travelling waves that we interpret as bodywaves. This interpretation is supported by records of local seismic events, and by numerical simulations (arrival times, polarization) in a crustal model which is derived from the results of the active seismic studies.

DATA AND SIGNAL PROCESSING

We analyse three component seismic data continuously recorded during the POLENET/LAPNET temporary experiment. We used only stations equipped with broadband sensors, and included several permanent broadband stations in our data-set. The array configuration (fig. 1) is approximately a 2D grid with station separations that span from ~50 km to ~600 km. The array was installed between spring and autumn 2007, for a duration of two years. We used records for the calendar year 2008 during which the array was fully

operational.

Pedersen et al. 2007 reported the presence of strong directivity of the noise field, especially observed from strong asymmetric surface waves signals on the noise correlations at intermediate frequencies (0.02-0.1 Hz) while the high frequency (0.1-1 Hz) part of the noise was distributed over larger azimuth ranges. Their study was limited to winter month, and the major part of high frequency energy was related with the sea activity along the eastern Atlantic coast. In our case, where the seismic array was installed for two years, the average of the correlations over one year (2008) in a frequency range from 0.1 and 2 Hz present an high signal to noise ratio over long distances (~ 600 km) and in both causal and acausal parts of the correlations as expected in a fully diffuse wave-field or in presence of randomly distributed sources.

The standard pre-processing included removing the data mean and trend, prefiltering, resampling to identical sampling rate and deconvolution of the instrumental responses. The noise correlations were calculated for all combinations of radial, transverse and vertical components, which required rotation of the horizontal components for each station pair according to the azimuth at each station of the great-circle between the two stations. To analyse broadband signals while removing the effects of earthquakes, we applied two supplementary steps before correlation. We firstly split the continuous data into four hour windows and removed the ones where amplitudes were present which were larger than 3 times the standard deviation of the signal. This step additionally reduces the effect of instrumental problems such as spikes. Secondly, we apply a spectral whitening in a frequency band from 0.1 to 2 Hz. This second step also diminishes the relative predominant contribution of surface waves related to the secondary microseismic peak at ~ 0.14 Hz.

After this processing the seismic noise traces are correlated for all couple of stations and stacked over one year, without applying 1-bit normalization. We verified the quality of

the correlations by comparing different processing procedures, including one where all major earthquakes were removed. In this test we used the correlations processed as described above. Then, using the earthquakes and explosions database of the Finnish seismological service, we removed all the time windows where earthquakes or explosions occurred and we stacked the correlations over one year. Since we study high frequency noise data (0.1-2 Hz), local seismicity can dramatically reduce the quality of the noise correlations (Bensen et al., 2007). We compared the correlations stack with and without local seismic events and we observed a stable reconstruction of all the seismic phases. From this observation we consider our processing procedure as sound and not significantly contaminated by quarry blasts and seismic events.

The bandpass filtered (0.5-2 Hz) noise correlations that have a signal to noise ratio larger than five are show in Figures 2, 3 and 4. The correlations are organized so that positive times correspond to waves propagating from the easternmost to the westernmost of the two stations. Out of the nine components of the correlations, we show the vertical-vertical (ZZ), radial-radial (RR) and transverse-transverse (TT) components, plotted as a function of the inter-station distance.

RESULTS AND DISCUSSION

In all the analysed components of the correlations we can identify coherent surface waves propagating from one station to another. The fundamental mode Rayleigh waves (Rg) portion of the estimated Green's function (EGF) are observed on both ZZ and RR correlation (fig. 2 and 3 respectively), with a propagation velocity of approximately 3 km/s. On the TT component (fig. 4) of the EGF we observe fundamental mode Love waves (L), with a velocity of ~ 3.5 km/s. Both Love and Rayleigh waves appear symmetrically on the seismic sections, which indicates either a good diffusivity of the noise-field or well distributed noise sources. The signal to noise ratio of these high-frequency surface waves remains high out to the full

distance range covered by the array, i.e. over up to 600 km.

We here wish to draw attention to other coherent phases that are clearly present in the seismic sections. Firstly, we note the coherent phase which is present on the ZZ components of the correlations (fig. 2) with an apparent velocity of approximately 3.5 km/s, which corresponds to expected apparent velocities for SmS waves, i.e. waves reflected at the Moho. These waves are stronger on the acausal part of the correlations, so they must originate in a different source or scatter distribution than the fundamental mode surface waves discussed above. This type of wave is not observed on the TT component, however such waves would be masked by the Love waves which also have velocities close to 3.5 km/s. Secondly, a signal with an apparent velocity of approximately 6 km/s, i.e. close to the expected apparent velocity of the PmP phase, is observed on the acausal part of the RR component. Frequency-time analysis shows that these two phases are non-dispersive over the frequency interval where they can be observed, which is 0.5-2 Hz. We can therefore, at this stage, hypothesize that these waves present in the noise correlations are body waves, and most likely SmS and PmP waves.

A first verification of whether the high velocity signals on the correlations are consistent with being body waves, we compare the noise correlations with earthquake data. We use the acausal part of the correlation traces of which we use only the ones with a signal to noise ratio higher than ten (in the body wave arrival windows). We choose a shallow local event ($M_L=2.9$) located beneath the northern part of the array (fig. 1) and for which clear signals are observed for the frequency band of interest (0.5-2 Hz). The earthquake data are preprocessed identically of the continuous noise recordings, and the horizontal components are rotated to obtain the radial and transverse components.

Figure 5 shows the seismic sections with the radial (5a, 5b) and vertical (5c, 5d) components of the noise correlations (blue) and earthquake records (black). The distance axis

corresponds to the inter-station distance for the noise correlations and the epicentral distance for the earthquake records. The earthquake data clearly show the fundamental mode Rayleigh waves on both radial and vertical components and the faster P and S wave on the radial and vertical components respectively. For the earthquake data, both single SmS and PmP are emerging from a distance of approximately 110km, which corresponds to approximately critical distance, however their amplitude is high from approximately 200km distance. SmS² is clearly observed from 280 km distance.

The comparison with earthquake data seems to give further evidence that the observed waves that arrive prior to the surface waves could indeed be body waves. Because the crustal model of the area is well known, and as the crustal model only varies very moderately beneath the study area, we can also directly compare the noise correlations with the numerical Green's functions calculated using a 1-D Earth model. We base our velocity model (see table 1) on the interpretation of HUKKA seismic reflection profiles as presented by Janik et al. (2007). The velocities of the upper crust are modified using the parameters obtained by Pedersen and Campillo (1991) who analysed high frequency Rayleigh waves from a quarry blast to obtain shear velocities and quality factor Q down to 3km depth. At larger depths we used Q values based on Uski et al. 1996. We calculate synthetic seismograms using the frequency-wavenumber method by Bouchon (1981), using a vertical point source located at the Earth's surface. The vertical and radial component seismograms, calculated at 100 points at 10km distance interval, correspond to the Green's function G_{ZZ} and G_{RR} which we need to compare to the Z-Z and R-R correlations.

The vertical and radial components of the correlations (blue) and synthetic seismograms (black) are shown in Figure 6. All the signals are filtered in the frequency range 0.5 to 1 Hz. The synthetic seismograms show dominant fundamental mode Rayleigh waves on the vertical component, as observed on the Z-Z correlations. The regularly spaced

synthetic vertical component seismograms clearly show the single and multiply Moho reflected S waves beyond the critical distance of ~ 110 km of SmS and up to distances of 350km. The velocity is similar to the one of the early waves in the Z-Z noise correlations, and the similarity is striking as to the pattern where the SmS² phase gradually become dominant over the SmS phase from 350km and beyond. Weak P waves can also be observed on the vertical component synthetic seismograms, with a velocity of approximately 6 km/s, as the ones observed on the Z-Z correlations. The signal to noise ratio on the correlations is however insufficient to easily detect them over the whole of the section. More evident are the P waves, observed on the RR correlations, that propagate with a velocity of ~ 6 km/s which is close to the velocity of the PmP phases observed on the RR synthetics seismograms.

The very successful comparison of the noise correlation sections with the earthquake records and the synthetic seismograms are strong arguments in favor of explaining the early arrivals in the noise correlations as body waves. A final argument resides in a strong similarity in polarizations of synthetic seismograms and noise correlations. The analysis of polarized seismic waves requires phase and amplitude informations of the seismic traces. Strong non linear pre-processing (as applied for noise correlation) can be a limitation, because their effect on the amplitude of the signals. Recent results (Cupillard et al., 2011, Prieto et al., 2011) demonstrate that standard pre-processing as one-bit or whitening have little effect on the amplitude informations of the noise correlation functions, so that attenuation can be obtained from the EGF (Prieto et al. 2011). From the previously cited works emerge that is possible perform polarization analysis using ambient noise, also if pre-processing was applied to the raw data.

Figure 7 b-c shows the particle motion observed for a correlation chosen for its high signal to noise ratio for a station couple located sufficiently far apart (211 km, station pair KIF-LP51) to separately analyse the participle motion of the Rayleigh waves and the two

early hypothesized body waves. We used the ZR and ZZ components of the noise correlations to obtain their particle motion and compare it with the one computed for a vertical force acting onto the Earth's surface. The particle motions are shown in three time windows, which correspond to the Rayleigh wave and the two hypothesized body waves.

The agreement between particle motion as observed on synthetic seismograms and noise correlations is striking. The Rayleigh waves have, as expected, an elliptical particle motion with very similar ratio between the ZR and ZZ axis. The PmP wave is linearly polarized, with a coefficient of rectilinearity ~ 0.9 (~ 1 on the synthetic polarization), and polarization angle of $\sim 52^\circ$ as compared to vertical, which is very similar to the $\sim 56^\circ$ observed on the synthetic motion. The SmS polarization is more complex due to free surface conversion. A linearly polarized SV wave incident at free surface beyond the critical conversion angle create phase shifted reflected SV wave and an evanescent P wave (Aki and Richards, 1980). The result of this sum of differently polarized waves can be observed in the synthetic seismograms as an inclined, elongated elliptic like polarization. Remarkably, the polarization on the noise correlations is in very good agreement with the synthetics also for these waves. This is a strong argument in favour of our interpretation of these waves as SmS.

CONCLUSION

The noise correlations from the northernmost part of the Baltic Shield are dominated by fundamental mode Rayleigh and Love waves. In addition to these waves, we observe coherent phases up to 500km inter-station distance which have an apparent velocity higher than the one observed for the fundamental mode surface waves. The fast waves are relatively high frequency (0.5-2Hz) and non-dispersive in that frequency range.

The comparison with earthquake records from a local event also showed the presence of these waves, and synthetic seismograms were also in excellent agreement with the noise

correlation. The synthetic seismograms very clearly points towards identifying the fast waves as single and multiply Moho reflected P and S waves, an interpretation which is supported by the wave polarization for different time windows. Note that the agreement between noise correlations and synthetic seismograms was dependent on the use of a crustal model based on active seismic studies (e.g. Janik et al., 2007), complemented with low S-wave and Q values in the uppermost crust as observed locally by Pedersen and Campillo (1991) along a 200km long profile south of the present study area to obtain similar surface/body wave amplitude ratios. A first conclusion of this study in terms of the local crustal structure is therefore that the low S-velocity and low Q model is widespread over the whole study area.

The conditions that need to be met for a successful and systematic use of body waves for lithospheric studies are still uncertain. The first issue is the minimum amount of data needed to observe the body wave contribution to the Green's function. Theoretically the correlation function converges to the complete Green's function as the square root of the time over which the correlation is evaluated. Such duration dependency is also present in our correlations, when we calculate the amplitude ration of the PmP phases and the remnant fluctuations for different durations of analysis. For the data at hand, good PmP arrivals with an acceptable Signal to Noise Ratio (SNR) are observed after just one month of time averaging. This suggests that travel time measurements can be performed even with limited reording duration.

The second issue is how the noise source distribution and its distance from the array affect the high frequency noise correlations. A previous study south of our study area (Pedersen et al., 2007) points towards the generation of the high-frequency seismic noise along the eastern Atlantic coastline during the winter season. This could potentially have a major impact on our observed noise correlations, and possibly explain the time asymmetry of the observed body waves. For such distant sources, two situations can be hypothesized.

247 Firstly, the presence of scattered energy from structures outside the study region can strongly
248 contribute to the convergence of the correlation to the Green's function by producing an
249 isotropic, equipartitioned field around the stations. If the stations considered are close
250 enough, and scattering and attenuation weak enough, ballistic waves can still be observed with
251 sufficient amplitude to emerge from the fluctuations. In a second situation, if the scattering
252 and attenuation are strong along the path between the two stations considered, the
253 identification of weak ballistic arrivals hidden in the correlation fluctuations will be
254 impossible. These issues are explored in Larose et al. (2008) who presented a heuristic model
255 for the SNR in correlations of signals considering specifically the role of scattering in
256 heterogeneous media. Note that the SNR is the ratio between actual Green function and the
257 remnant fluctuation level of the correlation. The SNR is expected to decrease with increasing
258 absorption and with distance. In presence of scattering, Larose et al. (2008) also showed that
259 the SNR is behaving following two regimes: SNR is increasing with scattering strength for
260 distances smaller than the transport mean free path l^* , while it is decreasing with scattering
261 strength for distance larger than l^* . This is in agreement with the fact that regional body
262 waves have so far been detected in cratons (Zhan et al., 2010, this study), characterized by
263 weak attenuation and large mean free path. In Finland, attenuation measurements for S wave
264 in the crust (Uski et al., 1996) suggest that the mean free path is at least on the order of the
265 aperture of the LAPNET network. Further work must be carried out to explore whether body
266 waves can be extracted for all types of crustal structure,.More precisely, in strongly
267 heterogeneous crustal structures, wave scattering could be sufficient to reduce the amplitude
268 of the body waves to a point where they would be hidden in the fluctuations of the correlation
269 functions. The result we report here is encouraging even though more work is required to
270 demonstrate whether our results can be generalized to other geological contexts to open the
271 possibility of the use of noise derived body waves for systematic imaging of the Earth's

interior.

ACKNOWLEDGEMENT

We greatly acknowledge support from the QUEST Initial Training network funded within the EU Marie Curie Programme. This study received supported from the ANR BegDy project, the Institut Paul Emil Victor, and European Research Council through the advanced grant “Whisper” 227507. We thank E. Larose for useful discussions. Synthetic seismograms were calculated using Computer Program in Seismology (Herrmann, R. B., 1996). The POLENET/LAPNET project is a part of the International Polar Year 2007-2009 and a part of the POLENET consortium, and received financial support from The Academy of Finland (grant No. 122762) and University of Oulu, ILP (International Lithosphere Program) task force VIII, grant No. IAA300120709 of the Grant Agency of the Czech Academy of Sciences, and the Russian Federation : Russian Academy of Sciences (programs No 5 and No 9). The Equipment for the temporary deployment was provided by: RESIF – SISMOB, FOSFORE, EOST-IPG Strasbourg Equipe sismologie (France), Seismic pool (MOBNET) of the Geophysical Institute of the Czech Academy of Sciences (Czech Republic), Sodankyla Geophysical Observatory (FINLAND), Institute of Geosphere Dynamics of RAS (RUSSIA), Institute of Geophysics ETH Zürich (SWITZERLAND), Institute of Geodesy and Geophysics, Vienna University of Technology (AUSTRIA), University of Leeds (UK). The POLENET/LAPNET working group consists of: Elena Kozlovskaya, Teppo Jämsen, Hanna Silvennoinen, Riitta Hurskainen, Helle Pedersen, Catherine Pequignat, Ulrich Achauer, Jaroslava Plomerova, Eduard Kissling, Irina Sanina, Reynir Bodvarsson, Igor Aleshin, Ekaterina Bourova, Evald Brückl, Tuna Eken Robert Guiguet, Helmut Hausmann, Pekka Heikkinen, Gregory Houseman, Petr Jedlicka, Helge Johnsen, Elena Kremenetskaya, Kari Komminaho, Helena Munzarova, Roland Roberts , Bohuslav Ruzek, Hossein Shomali,

297 Johannes Schweitzer, Artem Shaumyan, Ludek Vecsey, Sergei Volosov. We thank two
298 anonymous reviewers who helped to improve the manuscript.

299

REFERENCES

- Aki, K. & Richard, P.G., 1980, *Quantitative seismology-Theory and Methods*, W. H. Freeman, New York.
- Bensen, G.D., Ritzwoller, M.H., Barmin, M.P., Levshin, A. L., Lin, F., Moschetti, M. P, Shapiro, N. M. & Yang, Y., 2007, Processing seismic ambient noise data to obtain reliable broad-band surface wave dispersion measurement, *Geophys. J. Int.*, **169**, 1239-1260.
- Bouchon, M, 1981, A simple method to calculate green's functions for elastic layered media. *Bull. Seismol. Soc. of Am.*, **71**, 959–971.
- Campillo, M., 2006, Phase and Correlation in 'Random' Seismic Fields and the Reconstruction of the Green Function, *Pure Appl. Geophys.*, **163**, 475-502.
- Cupillard, P., Stehly, L. & B. Romanowicz, 2011, The one-bit noise correlation: a theory based on the concepts of coherent and incoherent noise. *Geophys. J. Int.*, **184**, 1397-1414.
- De Verdière, Y., 2011, A semi-classical calculus of the correlations, *Compte Rend. Geosc.*, In Press.
- Draganov, D., Campman, X., Thorbecke, J., Verdel, A., & Wapenaar, K., 2009, Reflection images from ambient seismic noise. *Geophysics*, **74**, 63–67.
- Gouédard, P., Stehly, L., Brenguier, F., Campillo, M., de Verdière, Y. C., Larose, E., Margerin, L., Roux, P., Sánchez-Sesma, F. J., Shapiro, N. M., & Weaver, R. L., 2008, Cross-correlation of random fields: mathematical approach and applications, *Geophys. Prospect.*, **56**, 375–393.
- Hennino, R, Trégourès, N., Shapiro, N. M., Margerin, L., Campillo, M., van Tiggelen, B. A. & Weaver, R. L., 2001, Observation of equipartition of seismic waves. *Phys. Rev. Lett*, **86**, 3447-3450.

323 Janik, T., Kozlovskaya, E & Yliniemi, J., 2007, Crust-mantle boundary in the central
 324 fennoscandian shield: Constraints from wide-angle p and s wave velocity models and new
 325 results of reflection profiling in Finland, *J. Geophys. Res.*, **112**.
 326 Kozlovskaya, E, Poutanen, M. & P. W. Group. POLENET/LAPNET- a multi-disciplinary
 327 geophysical experiment in northern fennoscandia during IPY 2007-2008, 2006,
 328 Geophysical research abstract.
 329 Larose, E., P. Roux, M. Campillo, A. Derode, 2008, Fluctuations of correlations and Green's
 330 function reconstruction: role of scattering, *J. Appl. Phys.* 103, 114907
 331 Pedersen, H & Campillo, M., 1991, Depth dependence of q beneath the Baltic shield inferred
 332 from modeling of short period seismograms, *J. Geophys. Res.*, **18**, 1755–1758.
 333 Pedersen H., Kruger, F & the SVEKALAPKO Seismic tomography, 2007, Influence of the
 334 seismic noise characteristics on noise correlations in the Baltic shield, *Geophys. J. Int.*, **168**,
 335 197-210.
 336 Ritzwoller, M. H., Lin F. & Shen, W., 2011, Ambient noise tomography with a large seismic
 337 array, *Compte Rend. Geosc.*, in press
 338 Roux, P, 2005a, P-waves from cross-correlation of seismic noise. *Geophys. Res. Lett.*, **32**.
 339 Roux, P., Sabra, K. G., Kuperman, W. A. & Roux, A., 2005b, Ambient noise cross correlation
 340 in free space: Theoretical approach, *J. Acoust. Soc. Am.*, **117**, 79-84.
 341 Prieto, G. A., Denolle, M. Lawrence, J. F. & Beroza, G. C., 2011, On the amplitude
 342 information carried by ambient seismic field, *Compte Rend. Geosc.*, In Press.
 343 Sabra, K. G., Gerstoft, P., Roux, P., Kuperman, W. A. & Fehler, M. C., 2005, Surface wave
 344 tomography from microseisms in southern California. *Geophys. Res. Lett.*, **32**.
 345 Shapiro, N. M. & Campillo, M., 2004, Emergence of broadband Rayleigh waves from

346 correlations of the ambient seismic noise, *Geophys. Res. Lett.*, **31**.
 347 Shapiro, N.M, Campillo, M., Stehly, L. & Ritzwoller, M. H., 2005, High-Resolution Surface-
 348 Wave tomography from ambient seismic noise. *Science*, **307**, 1615 –1618.
 349 Uski, M.,Tuppurainen, A., 1996, A new local magnitude scale for the Finnish seismic
 350 network, *Tectonophysics*, **261**, 23-37.
 351 Wapenaar, K. 2004, Retrieving the elastodynamic green's function of an arbitrary
 352 inhomogeneous medium by cross correlation. *Phys. Rev. Lett.*, **93**.
 353 Weaver, R. L. & Lobkis, O. I., 2001, Ultrasonics without a source: Thermal fluctuation
 354 correlations at MHz frequencies. *Phys. Rev. Lett.*, **87**.
 355 Yang, Y., Ritzwoller, M. H., Levshin, A. L. & Shapiro, N. M., 2007, Ambient noise rayleigh
 356 wave tomography across europe. *Geophys. J. Int.*, **168**, 259–274.
 357 Yao, H., Beghein, C. & van der Hilst, R. D., 2008, Surface wave array tomography in SE tibet
 358 from ambient seismic noise and two-station analysis - II. crustal and upper-mantle
 359 structure, *Geophys. J. Int.*, **173**, 205–219.
 360 Zhan, Z., Ni, S., Helmberger, D. V., & Clayton, R. W., 2010, Retrieval of moho-reflected
 361 shear wave arrivals from ambient seismic noise, *Geophys. J. Int.*, **1**, 408-420.

Figure 1: Map of the geometry of the POLENET/LAPNET array. The black circles correspond to the broad-band stations used in this study. The red square in the north-eastern corner of the array shows the location of the earthquake used to compare the signals with the correlations.

Figure 2: Cross correlations of vertical (ZZ) components stacked over 1 year (2008) plotted as a function of the inter-station distances in the 0.5-1 Hz frequency band. The correlation traces are organized so that the positive time axis corresponds to energy propagating from the easternmost to westernmost of the two stations. Rg indicates Rayleigh waves, SmS indicates the waves that we interpret as S waves reflected from the Moho discontinuity (both first and second reflection).

Figure 3: Cross correlations of radial (RR) components stacked over 1 year (2008) plotted as function of the inter-station distances in the 0.5-1 Hz frequency band. The correlation traces are organized so that the positive time axis corresponds to energy propagating from the easternmost to westernmost of the two stations. Rg indicates Rayleigh waves, and PmP indicates the waves that we interpret as P waves reflected from the Moho discontinuity.

Figure 4: Cross-correlations of transverse (TT) components stacked over 1 year (2008) plotted as function of the inter-station distances in the 0.5-1 Hz frequency band. The correlation traces are organized so that the positive time axis corresponds to energy propagating from the easternmost to westernmost of the two stations. L indicates Love waves.

Figure 5: Comparison of the acausal part of (a) ZZ and (c) RR cross correlations plotted as

function of inter-station distances and (b) vertical, (d) radial component earthquake data plotted as function of epicentral distances. All the signals are filtered between 0.5 and 1 Hz. SmS and SmS2 indicate respectively the first and second S wave Moho reflection, while PmP indicates the P waves Moho reflection and Rg the Rayleigh waves.

Figure 6: Comparison of the acausal part of the (a) ZZ, (c) RR cross correlations plotted as function of inter-station distances. b) shows the vertical component (Z) of synthetic seismograms using a vertical point force (VF). d) shows the the radial component (R) of synthetic seismograms using a horizontal point force (HF) at the surface. All the signals are filtered between 0.5 and 1 Hz. The naming of the waves is the same as in previous figures.

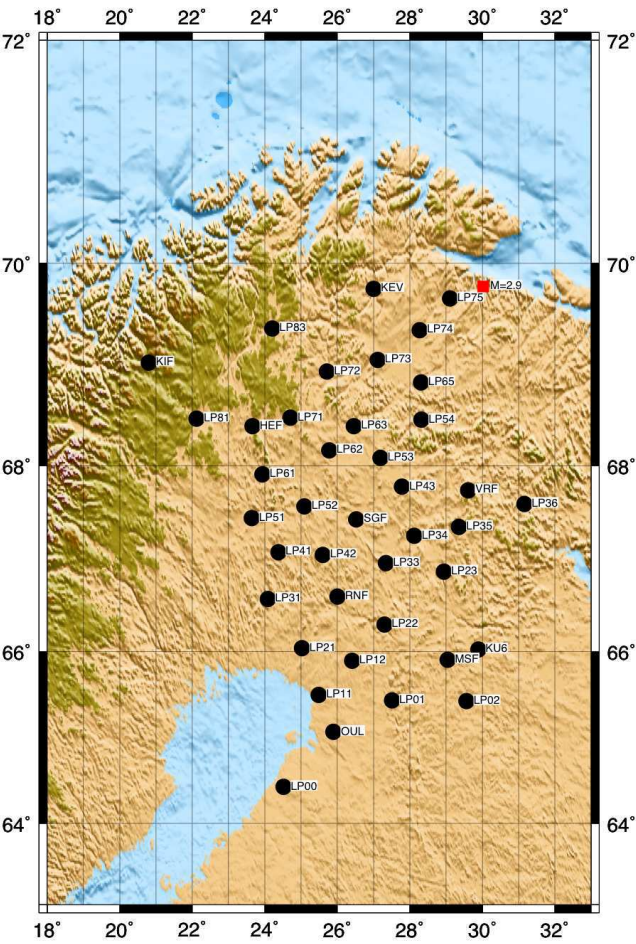
Figure 7: a) particle motion analysis for the cross-correlation between the station KIF-LP51, ZZ is the vertical-vertical correlation, ZR is the vertical radial correlation. Red line on the PmP particle motion analysis shows the result of the linear regression of the ZZ and ZR motion, the coefficient of linearity is 0.87 and the polarization angle is 52° to vertical. b) particle motion analysis for synthetic seismograms calculated for the same distance between the station KIF-LP51, ZVF is the vertical synthetic seismogram generated using a vertical point source at the Earth surface, RVF is the radial synthetic seismogram generated using a vertical point source at the Earth surface. The red line on the PmP particle motion analysis is the linear regression of the ZVF and RVF motion, the coefficient of linearity is 0.99 and the polarization angle is 56° to vertical.

Table 1 : Crustal model used to calculate the synthetics seismograms. V_p is the P wave velocity, V_s is the S waves velocity, Q_p is the P waves quality factor and Q_s is the S

410 waves quality factor.

411

412



413

414

415

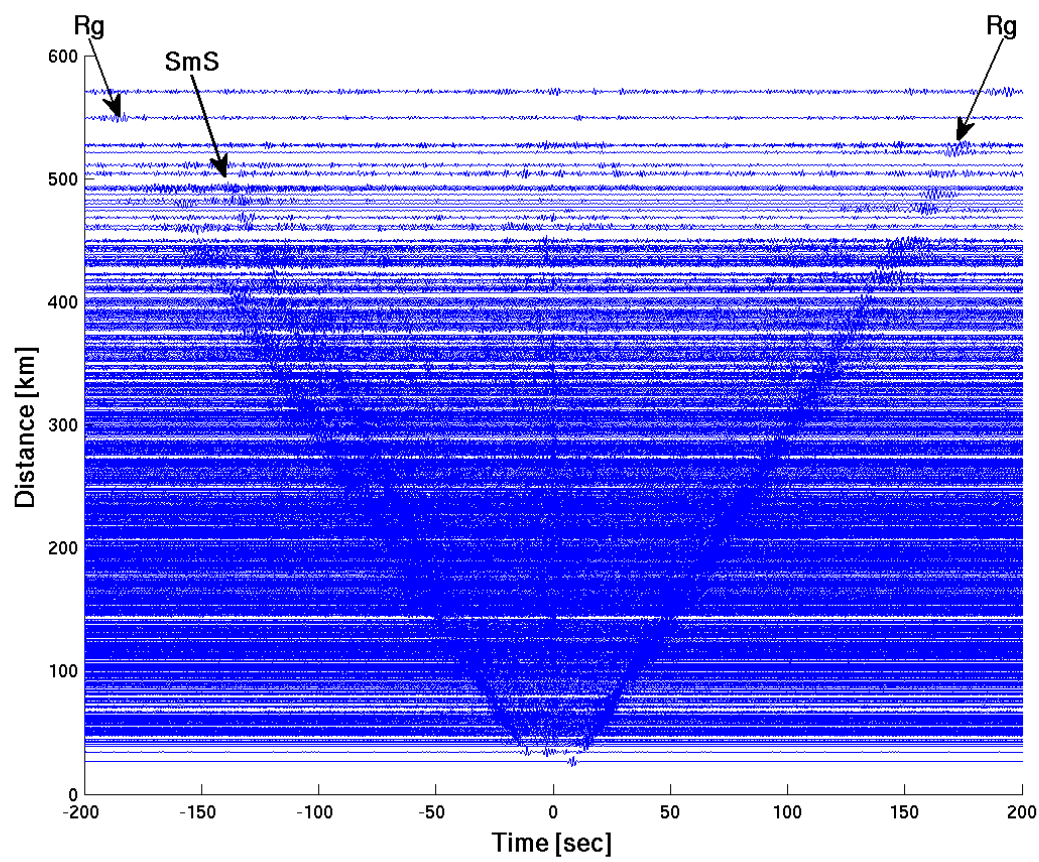
416

417

418

Figure 1

419



420

421

Figure 2

422

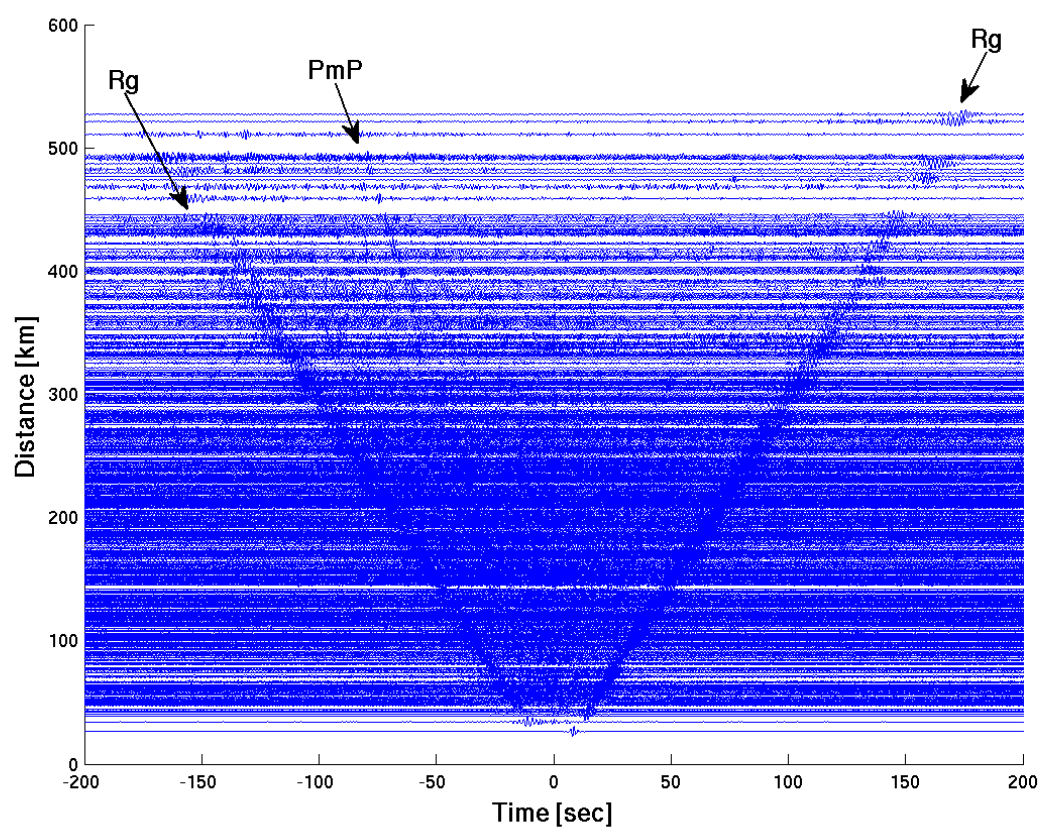


Figure 3

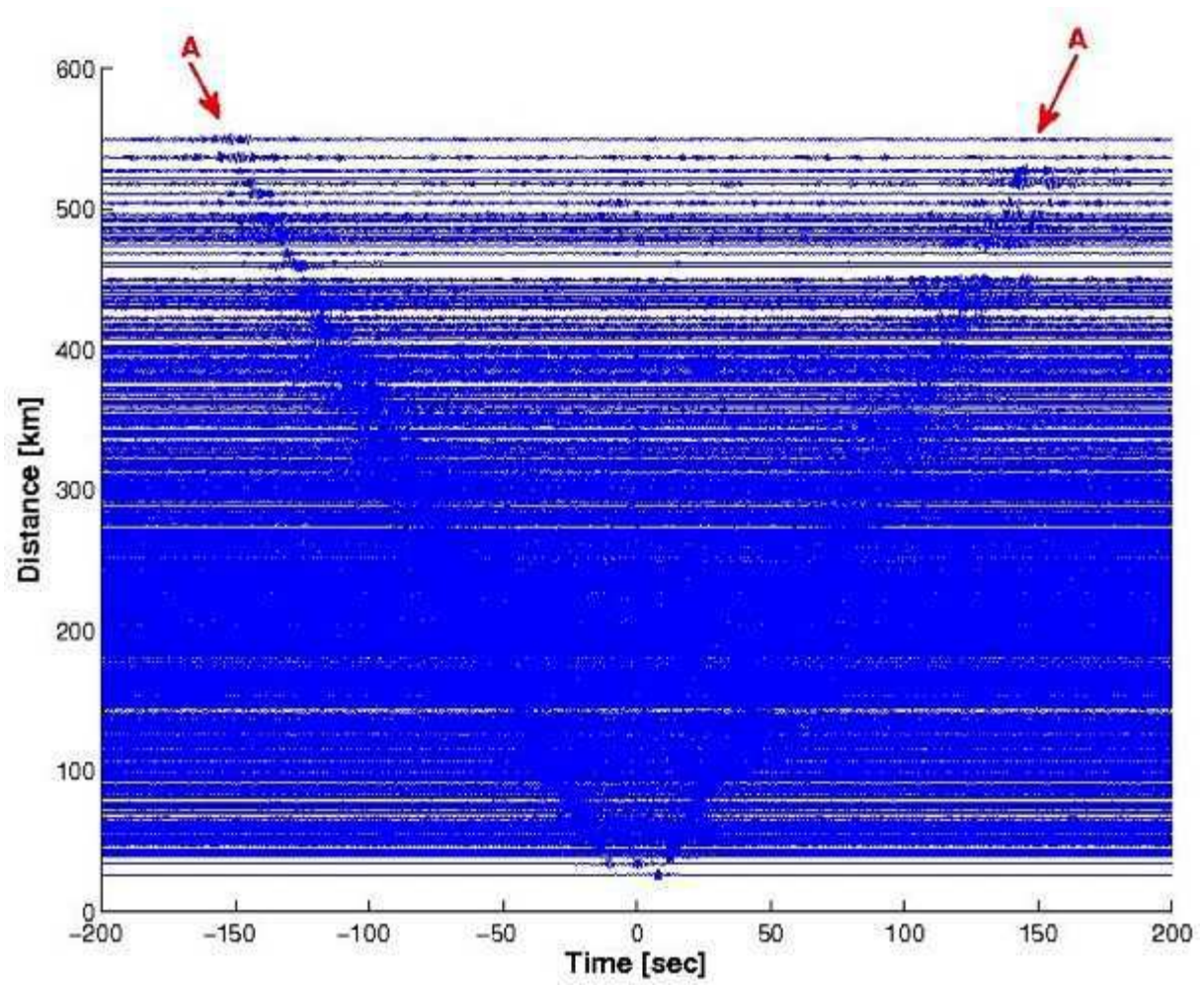
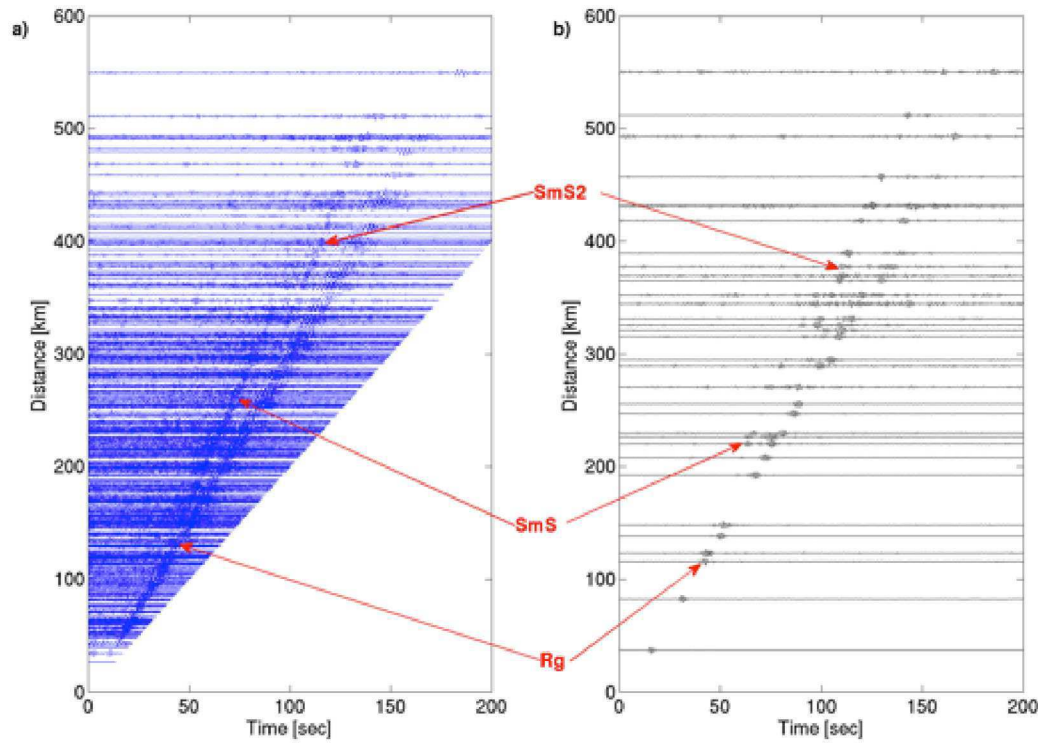
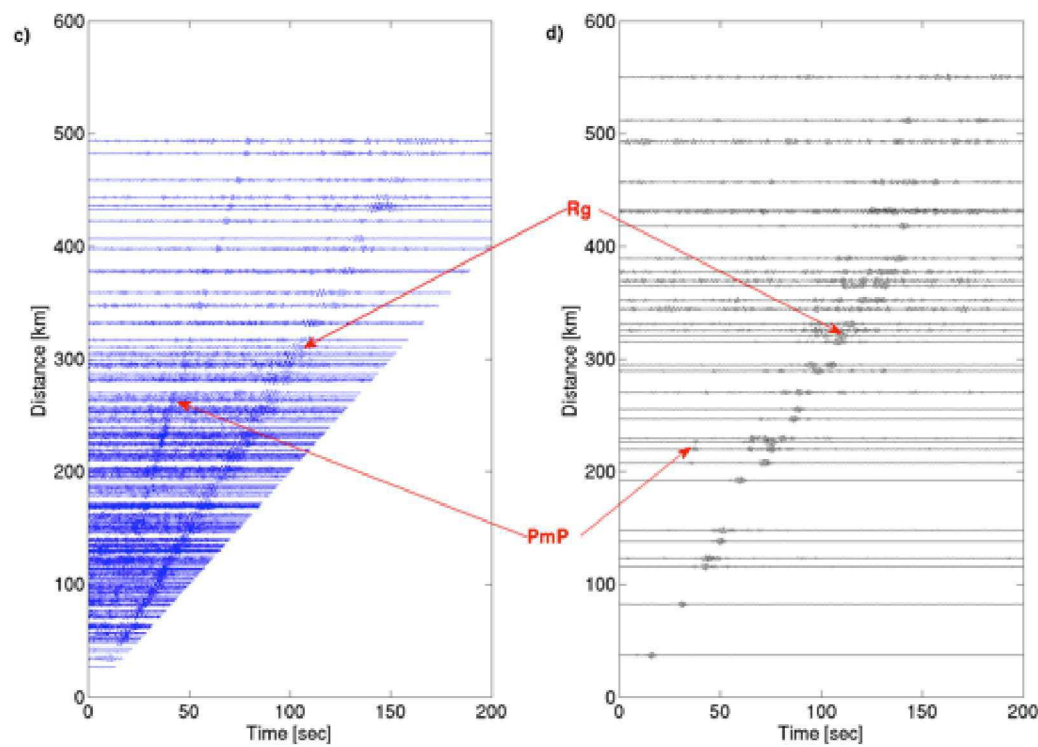
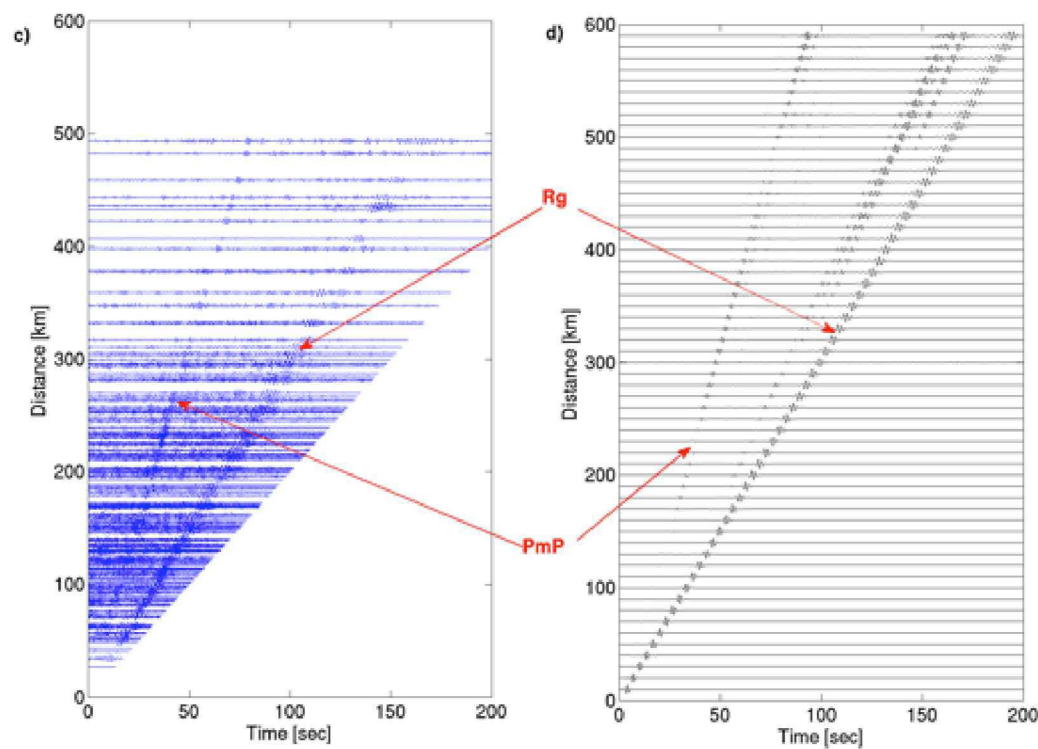


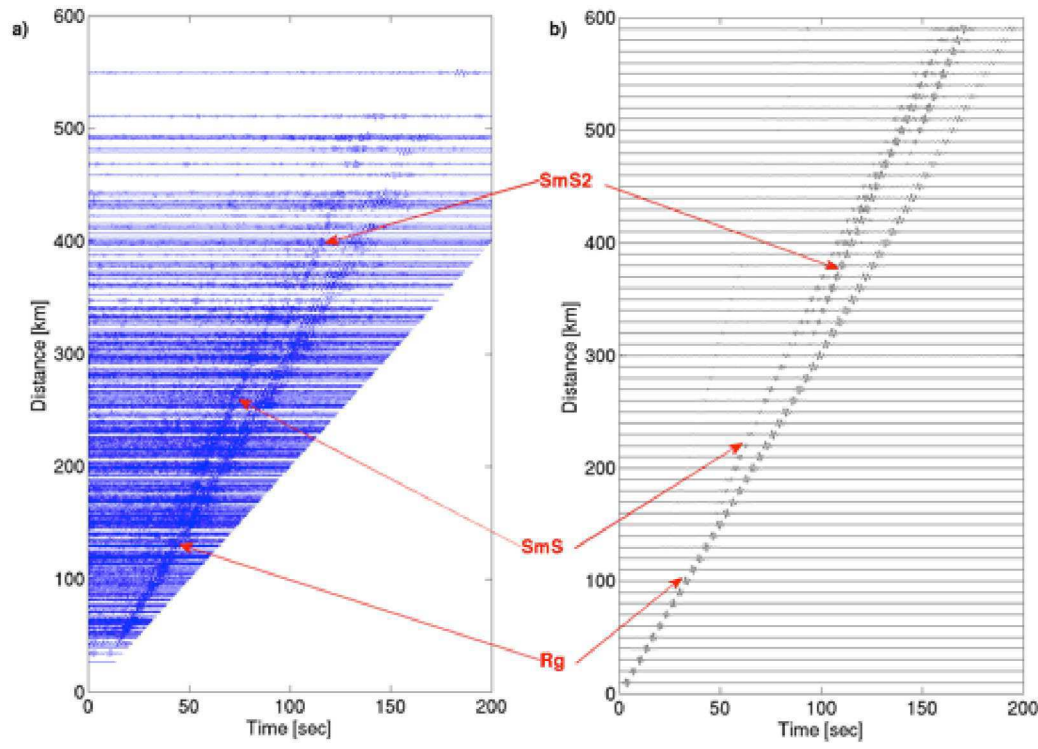
Figure 4



434



435

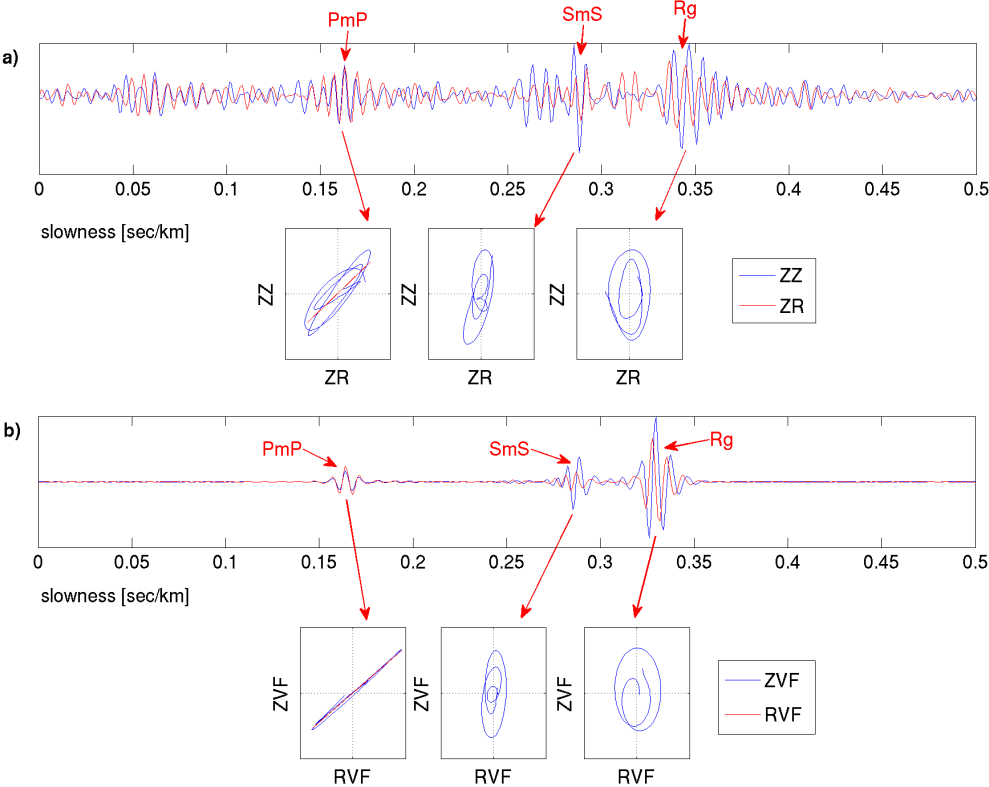


436

437

Figure 6

439



440

441

Figure 7

442

443

444

Table 1

Depth (km)	Vp (km/s)	Vs (km/s)	Qp	Qs
0	5.85	3.40	1000	100
3	6.30	3.65	1000	1000
18	6.60	3.85	1000	1000
38	7.15	4.00	1000	1000
40	7.40	4.06	1000	1000
44	8.03	4.62	1000	1000

445

